Crystal structure and magnetic properties of ternary Al_3CoNd_2 compound

Liuqing Liang,[1,2] Degui Li,[1,2,a)] Chenzhong Jia,[1,2] and Ming Qin[1,2]
[1]School of Material Science and Engineering, Baise University, Baise, Guangxi 533000, China
[2]Engineering Research Center of Advanced Aluminium Matrix Materials of Guangxi Province, Baise University, Baise, Guangxi 533000, China

(Received 5 April 2021; accepted 7 July 2021)

A ternary compound Al_3CoNd_2 was synthesized and its crystal structure parameters were determined by the Rietveld refinement method based on powder X-ray diffraction data. Results show that the compound crystallizes in the $MgCu_2$-type structure (cubic Laves C15 phase, space group $Fd\bar{3}m$), with the lattice parameter of $a = 7.8424(2)$ Å, unit-cell volume of $V = 482.33$ Å^3, and calculated density of $D_{calc} = 5.90$ g.cm^{-3}. The residual factors converge to $R_p = 0.1024$ and $R_{wp} = 0.1287$. The reference intensity ratio value obtained experimentally is 3.03. Magnetic susceptibility measurements indicate an agreement with the Curie–Weiss law in the temperature range of 385–450 K, and paramagnetic Curie temperature of $\theta_p = 379.9$ K. Both rare-earth elements and cobalt ions contribute to the paramagnetic moment. The saturation magnetic moment and magnetic hysteresis loop were measured for the Al_3CoNd_2 compound at various temperatures. Results show that the saturation magnetic moment value decreases with an increase in temperature and the compound becomes a ferromagnet below the Curie temperature T_c. [doi:10.1017/S0885715621000476]

Key words: crystal structure, powder XRD, Rietveld refinement, Al_3CoNd_2, magnetization measurement

I. INTRODUCTION

In the past few decades, Laves phases with AB_2 compositions have been employed in many important and attractive applications, such as superconducting materials, giant magnetostrictive materials, hydrogen storage materials, and high-temperature structural materials, owing to their excellent physical and chemical properties (Strnat and Strnat, 1991; Szytula and Leciejewicz, 1994; Tao *et al.*, 2008). For instance, binary rare-earth Laves phase $NdAl_2$ (Gschneidner and Calderwood, 1989) that crystallizes in the cubic $MgCu_2$-type structure C15 phase has been reported. The crystal and magnetic properties of $NdAl_2$ have been investigated by Nereson *et al.* (1966) using neutron diffraction and susceptibility measurements. The results showed Curie–Weiss behavior in the paramagnetic region and the compound was basically ferromagnetic below Curie temperatures. Another Laves phase compound $NdCo_2$ has been investigated by Xiao *et al.* (2006). The compound was investigated using the Rietveld refinement technique based on high-resolution neutron powder diffraction data. Detailed information pertaining to the crystal and magnetic structures of $NdCo_2$ at different temperatures was reported. Furthermore, a study showed that adding a third group member, such as B, Al, or Ga, to an R–T (R = rare-earth, T = transition element) alloy and adjusting its chemical composition can significantly improve the magnetic properties of the material (Weitzer *et al.*, 1989). Therefore, R–Co–Al ternary intermetallic compounds and their remarkable physical properties have attracted the attention of many researchers.

To our best knowledge, the ternary compounds Nd_4CoAl, $Nd_2Co_6Al_{19}$, and $Nd_{13}Co_{14-x}Al_{4+x}$ have been reported and their crystal structures have been investigated by Riani *et al.* (2020). Moreover, several other ternary compounds have already been reported in the literature. For example, Nd_6Co_2Al was synthesized by Stegemann and Janka (2018). Its unit-cell parameters were refined via powder X-ray diffraction (XRD) experiments. $NdCo_2Al_8$ was studied by He *et al.* (2009) using the Rietveld refinement method to determine its crystal structure parameters. The Nd_2Co_2Al structure was investigated by Pani *et al.* (2002) via single-crystal and powder XRD. The structure and magnetic properties of $Nd_7Co_6Al_7$ were investigated by Yarmolyuk *et al.* (1986) and Canepa *et al.* (2000). They stated that this compound undergoes a ferromagnetic transition at 15.5 K. $NdCoAl_4$ and $Nd_2Co_3Al_9$ were refined by Tougait and Noël (2006) based on single-crystal XRD data. Their magnetic susceptibility measurements revealed an antiferroelectric ordering at low temperatures.

In our investigation of the title compound in the R–Co–Al system, Al_3CoNd_2 was synthesized in an argon-filled nonconsumable arc furnace and subjected to vacuum thermal annealing at 923 K for 4 weeks. In this study, we report our experimental results of the synthesis and Rietveld refinement results of the crystal structure and magnetic properties of Al_3CoNd_2.

II. EXPERIMENTAL

A sample of the ternary compound Al_3CoNd_2 was prepared by melting high-purity metals of Al, Co, and Nd in an arc furnace under an argon atmosphere (Liang *et al.*, 2013).

a)Author to whom correspondence should be addressed. Electronic mail: lidegui354@163.com

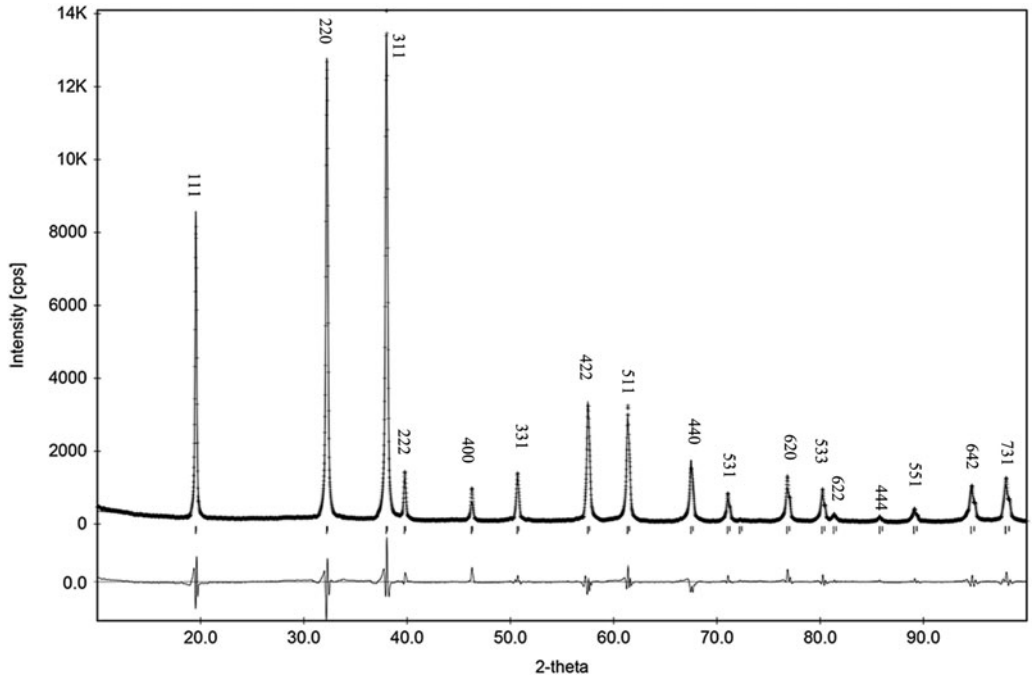

Figure 1. X-ray powder diffraction patterns for Al_3CoNd_2. "+" symbols represent observed patterns, the solid line represents the calculated patterns, "|" symbols represent the possible positions of Bragg reflections, and the bottom curve represents the difference between the observed and calculated patterns.

All the raw materials were flaky, and the purity of all the elements was 99.99%. The cooled buttons were flipped and remelted three times to achieve homogeneity. The mass loss after arc melting was less than 0.5 wt.%. After melting, the sample was thermally treated for 4 weeks at 973 K in an evacuated quartz tube. The sample was ground in an agate mortar and pestle to particle sizes of no greater than 20 μm. The powder XRD patterns for the Al_3CoNd_2 compound were collected at room temperature using a powder X-ray diffractometer (Smart Lab (9), Rigaku Corporation). The 300-mm radius diffractometer was equipped with Cu$K\alpha$ radiation ($\lambda = 1.54060$ Å) and a graphite monochrometer. The operating voltage and current were 40 kV and 150 mA. The 2θ scan range was from 10° to 100° with a step size of 0.02° and a count time of 2 s per step. Finally, 50 wt.% Al_3CoNd_2 and 50 wt.% corundum were prepared to determine the reference intensity ratio (RIR) value (Walter and Schreiner, 1995).

A powder sample of 18.5 mg was used for magnetic measurements. The magnetic susceptibility of the Al_3CoNd_2 compound was measured on a Quantum Design SQUID physical property measurement system (PPMS-9#VSM) in the temperature range of 2–450 K under an applied field of 50 Oe. Moreover, the field-dependent data of the saturation magnetic moment and magnetic hysteresis loop for the compound were measured at 2, 5, 10, 150, and 300 K under applied fields of up to 6.5 T.

III. RESULTS AND DISCUSSION

A. Structural refinement results and discussion

The Al_3CoNd_2 compound was verified via powder XRD analysis using the program JADE 6.0 (Materials Data Inc., 2002). The powder XRD patterns for the Al_3CoNd_2 compound were successfully indexed based on the cubic lattice. The reflection conditions, reflection intensities, and calculated lattice parameters proved that the compound is isostructural with Al_2Nd and crystallizes in the $MgCu_2$-type structure (cubic Laves C15 phase) with a space group of $Fd\bar{3}m$ (No. 227). The atomic positions of the elements were selected as a starting model for the Rietveld refinement using the DBWS9807a program (Young *et al.*, 2000). The pseudo-Voigt function was used to simulate the peak shapes. The lattice parameters were obtained using JADE 6.0. During the refinement process, the DMPLOT program (Marciniak and Diduszko, 1997) was used to record the refinement results. Figure 1 shows the observed, calculated data, and residuals of the powder XRD patterns of Al_3CoNd_2. Details of the refinement are summarized in Table I. After the refinement of 23 parameters, including the sample shift, scale factor, lattice constants, full width at half maximum, preferred orientation, thermal parameters, occupancy, and background parameters, the residual factors converged to $R_p = 0.1024$ and $R_{wp} = 0.1287$. Table II summarizes the final results for

TABLE I. Rietveld refinement data of Al_3CoNd_2.

Formula	Al_3CoNd_2
Space group	$Fd\bar{3}m$ (No. 227)
Radiation wavelength Cu$K\alpha_1$ (Å)	1.5405981
Unit-cell parameters (Å)	$a = 7.8424(2)$ Å
Unit-cell volume (Å^3)	482.33
Calculated density (g.cm^{-3})	5.90
Formula units per unit cell	$Z = 4$
Scan range	$10° \le 2\theta \le 100°$
Residual values	
R_p	0.1024
R_{wp}	0.1287
$R_{expected}$	0.0560
S	2.30

$$R_P = \frac{\sum |Y_i(\text{obs}) - Y_i(\text{calc})|}{\sum Y_i(\text{obs})}, \quad R_{WP} = \left\{ \frac{\sum \omega_i [Y_i(\text{obs}) - Y_i(\text{calc})]^2}{\sum \omega_i [Y_i(\text{obs})]^2} \right\}^{1/2}.$$

https://doi.org/10.1017/S0885715621000476 Published online by Cambridge University Press

TABLE II. Atomic coordinates, occupancy, and thermal parameters for Al_3CoNd_2.

Atom	Position	X	Y	Z	Occ.	B (nm^2)
Al	16c	0	0	0	0.74 (5)	0.038 (5)
Co	16c	0	0	0	0.26 (5)	0.038 (5)
Nd	8b	0.375	0.375	0.375	1	0.005 (5)

TABLE III. Interatomic distances in the crystal structure of Al_3CoNd_2.

Atom	Neighbor atoms	Distance (nm)	Atom	Neighbor atoms	Distance (nm)
Nd	Nd × 4	0.339 (5)	M	M × 6	0.277 (3)
	M × 12	0.325 (1)		Nd × 6	0.325 (1)

M = 74%Al + 26%Co.

the atomic coordinates, occupancy, and thermal parameters. Al and Co atoms occupy the same positions, and their occupancies are 0.74 and 0.26, respectively. The uncertainty for the occupancies is 0.05. Table III lists the selected interatomic distances for the Al_3CoNd_2 compound. The interatomic distances of Nd–Nd, M–Nd, and M–M atoms are all close to the sum of their metallic radii ($r_{Nd} = 0.181$ nm, $r_{Co} = 0.135$ nm, and $r_{Al} = 0.143$ nm). Figure 2(a) shows the Al_3CoNd_2 structure, indicating that the number of atoms per unit cell is 24 and the formula units per unit cell, $Z = 4$. The coordination environments of M and Nd are presented in Figures 2(b) and 2(c), respectively. Where M is the atomic position of 16c. Each M atom is surrounded by 6 Nd and M. Each Nd atom is surrounded by 4 Nd and 12 M.

B. Reference intensity ratio

To quantitatively analyze the phase in the future, the *RIR* value of Al_3CoNd_2 was calculated using the I/I_c method (Snyder, 1992). I/I_c is defined as the ratio of the intensity of the strongest line of an analyte to the corundum (113) line when the analyte is mixed at 50:50 by weight with corundum. Therefore, the powder XRD patterns for a mixture comprising

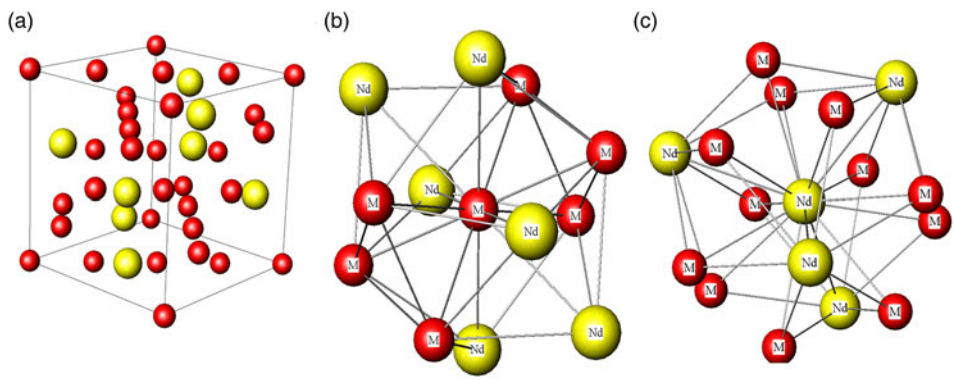

Figure 2. Structure and coordination environments of Al_3CoNd_2. (a) Al_3CoNd_2 structure, (b) M atom (74% Al and 26% Co), and (c) Nd atom.

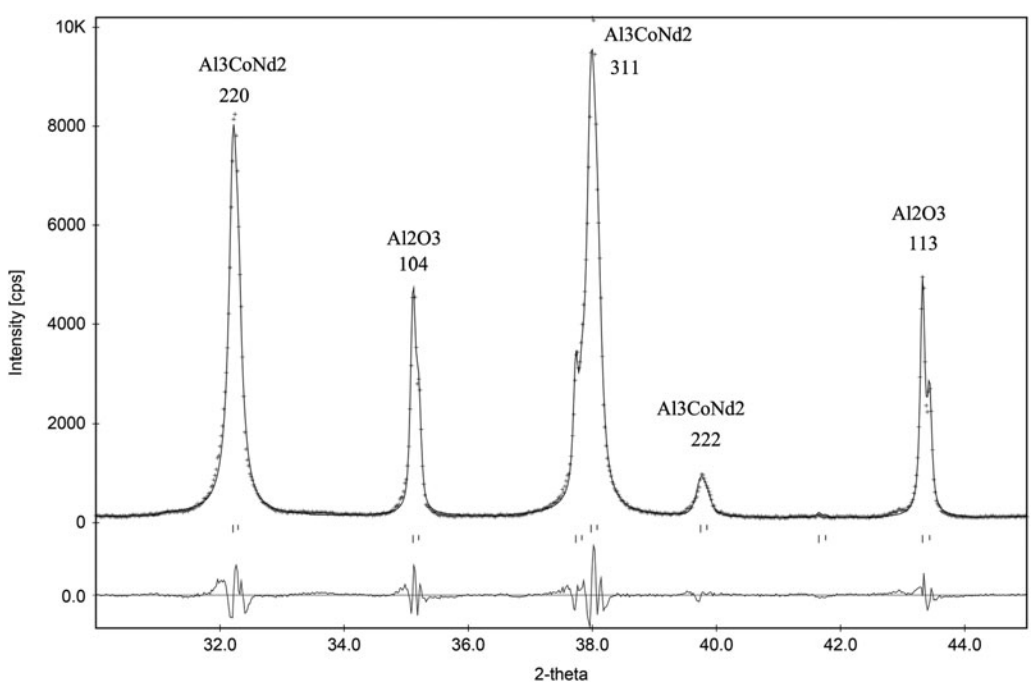

Figure 3. Low 2θ portions of the powder XRD pattern of 50 wt.% Al_3CoNd_2 and 50 wt.% corundum.

https://doi.org/10.1017/S0885715621000476 Published online by Cambridge University Press

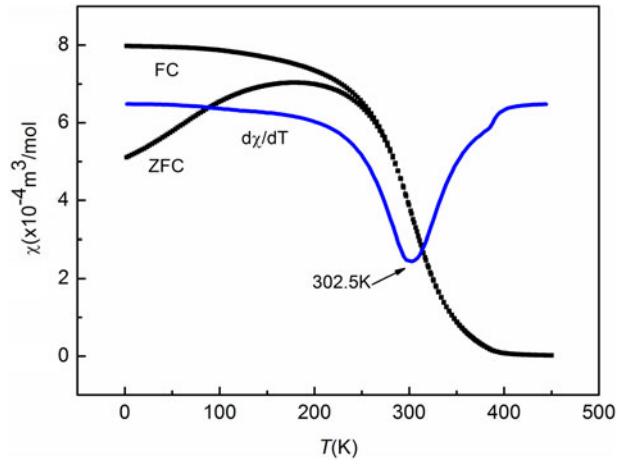

Figure 4. Temperature dependence of the magnetic susceptibility for Al_3CoNd_2.

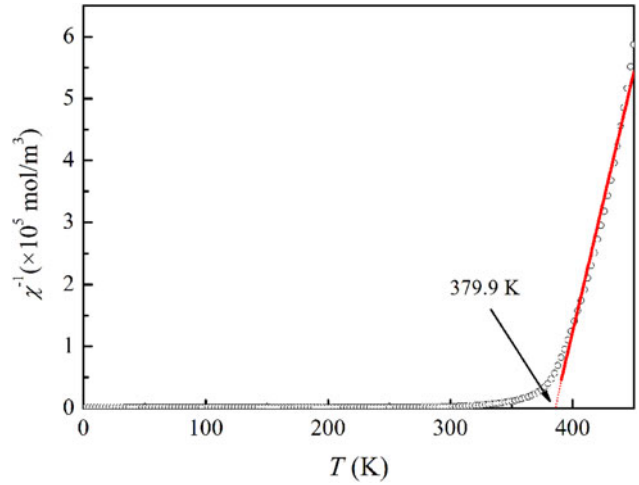

Figure 5. Reciprocal of the magnetic susceptibilities (x^{-1}) of the Al_3CoNd_2 compound. The red solid line represents the fit to the experimental data based on the Curie–Weiss law and circles represent the reciprocal of the magnetic susceptibilities.

50 wt.% Al_3CoNd_2 and 50 wt.% corundum were measured, as shown in Figure 3. However, the main peak for the compound at $2\theta = 38.018°$ overlaps another Al_2O_3 peak. Therefore, the Rietveld refined structure parameters were used to calculate the RIR value (Chung, 1974; Hubbard and Snyder, 1988), which is 3.03 based on the simulated structure data. This value is slightly smaller than the value obtained after adding Al_2O_3 powder, i.e., 3.23.

C. Magnetic properties

The temperature dependence of the magnetic susceptibility measured in an applied field of 50 Oe is plotted in Figure 4. The associated field-cooled/zero field-cooled (FC/ZFC) was observed at 280 K. Furthermore, the Curie temperature T_c identified as the minima in the first derivative of the χ–T curves is 302.5 K (Zeng *et al.*, 2007). Figure 5 shows the reciprocal of the magnetic susceptibilities as a function of the temperature for the compound. In the temperature range of 385–450 K, the linearity of the curve indicates agreement with the Curie–Weiss law:

$$1/\chi = (T - \theta_p)/C \tag{1}$$

where χ is the magnetic susceptibility, C is the Curie constant, and T is the temperature. The paramagnetic Curie temperature of $\theta_p = 379.9$ K was obtained by extrapolating the linear $1/\chi$. The effective magnetic moment of $\mu_{eff} = 6.57\ \mu_B$ per Nd^{3+} was calculated using the following formula (Koch and Strydom, 2008):

$$\mu_{eff} = \sqrt{\frac{3\kappa_B \chi (T - \theta_p)}{N_A \mu_0}} \tag{2}$$

where N_A is the Avogadro number, k_B is the Boltzmann constant, μ_B is the Bohr magneton, and μ_0 is the permeability of vacuum. The effective magnetic moment value is larger than the theoretical effective magnetic moment of $\mu_{eff} = 3.62\ \mu_B$ per Nd^{3+}, obtained using the following formula (Taylor and Darby, 1972; Lu *et al.*, 2011):

$$\mu_{eff} = g\sqrt{J(J+1)}\mu_B \tag{3}$$

where J is the angular momentum quantum number and g is

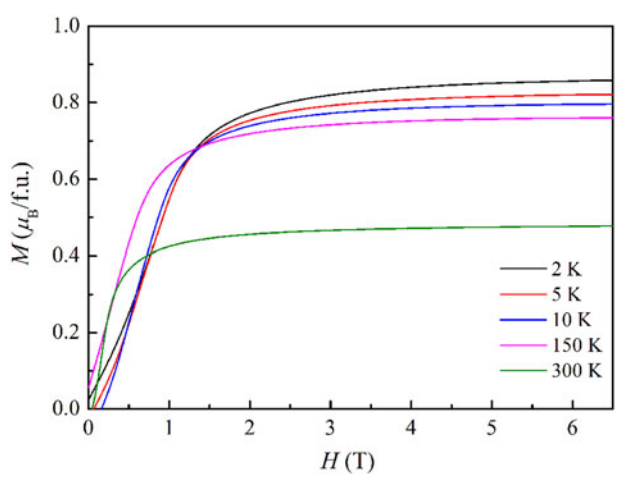

Figure 6. Isothermal magnetization curves (M–H) measured at various temperatures for the Al_3CoNd_2 compound.

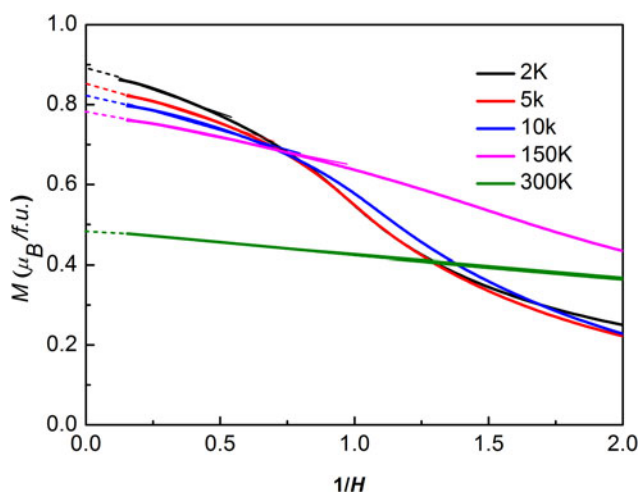

Figure 7. Isothermal magnetization curves ($M - (1/H)$) measured at various temperatures for the Al_3CoNd_2 compound.

https://doi.org/10.1017/S0885715621000476 Published online by Cambridge University Press

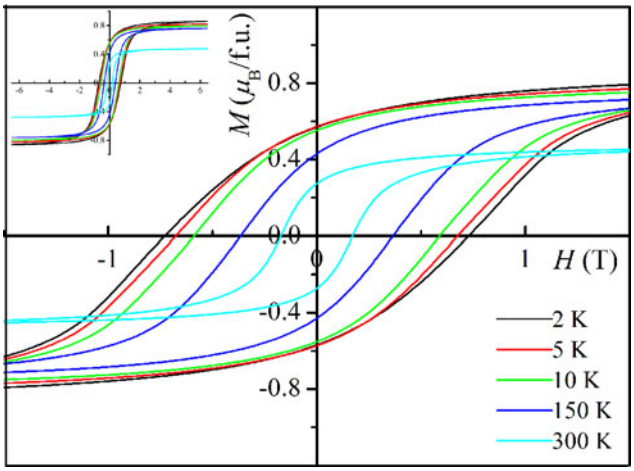

Figure 8. Magnetic hysteresis loop curves for the Al_3CoNd_2 compound at various temperatures.

the Lander factor. This indicates that both rare-earth elements and cobalt ions contribute to the paramagnetic moment.

To further explore the magnetism of the compound, magnetization measurements were performed at various temperatures. Figure 6 shows the isothermal magnetization curves (M–H) measured under the applied field of 0–6.5 T and at 2, 5, 10, 150, and 300 K. Full saturation is not achieved at the applied field of up to 6.5 T. Therefore, the empirical formula (Dai and Qian, 2017) is used

$$M_H = M_S\left(1 - \frac{\alpha}{H}\right) \tag{4}$$

where M_H is the corresponding magnetization under the applied field of H and α is a constant, to plot several curves for determining the saturation magnetization M_S (Figure 7) and extrapolating the linear part of the curve to the plot $(1/H) = 0$; consequently, the M_S value was obtained. Obviously, the maximum saturation magnetic moment at 2 K is 0.89 μ_B/f.u. and this value decreases with an increase in temperature. Figure 8 shows the magnetic hysteresis loop curves of the compound at various temperatures. Weak ferromagnetism is observed at 300 K and a hysteresis with a remnant magnetization M_r of 0.27 μ_B/f.u. and a coercive field H_c of 0.17 T is seen, which continues to enlarge as the temperature is reduced. At 2 K, M_r of 0.57 μ_B/f.u. and H_c of 0.73 T. Compared with the magnetic hysteresis loop at 2 K, Al_3CoNd_2 is a softer ferromagnet at a higher temperature. This implies that the compound is a ferromagnet below the Curie temperature T_c.

IV. CONCLUSION

In summary, the crystal structure of the Al_3CoNd_2 compound was determined by the powder XRD technique and structural refinement was performed using the Rietveld method. The compound is isostructural with Al_2Nd and crystallizes in the $MgCu_2$-type structure (cubic Laves C15 phase), with a space group of $Fd\bar{3}m$ (No. 227), a lattice parameter of $a = 7.8424(2)$ Å, and a unit-cell volume of $V = 482.33$ Å^3. The residual factors converge to $R_p = 0.1024$ and $R_{wp} = 0.1287$. The *RIR* value obtained experimentally is 3.03. The magnetic susceptibility curves follow the Curie–Weiss law in the temperature range of 385–450 K and the paramagnetic Curie temperature of $\theta_p = 379.9$ K. The saturation magnetic moment and magnetic hysteresis loop for the compound were measured at various temperatures. The results show that the saturation magnetic moment value decreased with an increase in temperature and the compound is a ferromagnet below the Curie temperature T_c.

V. DEPOSITED DATA

CIF and/or RAW data files were deposited with ICDD. You may request this data from ICDD at info@icdd.com.

ACKNOWLEDGEMENTS

The authors gratefully acknowledge the support from the National Natural Science Foundation of China (No. 51861001), the Guangxi Natural Science Foundation (No. 2018GXNSFAA138133 and 2016GXNSFDA380024), and the International Centre for Diffraction Data (No. 16-03).

Canepa, F., Manfrinetti, P., Palenzona, A., Cirafifici, S., Merlo, F., and Cimberle, M. R. (**2000**). "Ferromagnetic interactions in $Nd_7Co_6Al_7$," Intermetallics **8**, 267–272.

Chung, F. H. (**1974**). "Quantitative interpretation of X-ray diffraction patterns. I. Matrix-flushing method of quantitative multi-component analysis," J. Appl. Crystallogr. **7**, 519–525.

Dai, D. and Qian, K. (**2017**). *Ferromagnetism* (Science Press, Beijing).

Gschneidner, K. A. and Calderwood, F. W. (**1989**). "The AI–Nd (aluminum-neodymium) system," Bull. Alloy Phase Diagrams **10**(1), 28–30.

He, W., Zhong, H., Liu, H., Zhang, J., and Zeng, L. (**2009**). "Structure and electrical resistivity of $NdCo_2Al_8$," J. Alloys Compd. **467**, 6–9.

Hubbard, C. R. and Snyder, R. L. (**1988**). "Reference intensity ratio measurement and use in quantitative XRD," Powder Diffr. **3**, 74–78.

JADE Version 6.0 (**2002**). XRD *Pattern Processing* (Materials Data Inc., Livermore, CA).

Koch, N. E. and Strydom, A. M. (**2008**). "Electronic and magnetic properties of the rare earth intermetallic compounds RRu_4Sn_6 (R=Nd, Sm, Gd, Tb, Dy and Ho)," J. Magn. Magn. Mater. **320**, e128–e131.

Liang, L., Zeng, L., Liu, S., and He, W. (**2013**). "Crystal structure, thermal expansion and electrical properties of $GdCo_{0.67}Ga_{1.33}$ compound," Physica B **426**, 35–39.

Lu, X., Zeng, L., and Shih, K. (**2011**). "Crystal structure, thermal expansion and magnetic properties of $Pr_2Cu_{0.8}Ge_3$ compound," Mater. Chem. Phys. **130**, 1336–1340.

Marciniak, H. and Diduszko, R. (**1997**). *DMPLOT: Plot View Program for Rietveld Refinement Method, Version 3.38* (Computer Software) (High Pressure Research Center, Warsaw, Poland).

Nereson, N., Olsen, C., and Arnold, G. (**1966**). "Magnetic properties of $DyA1_2$ and $NdA1_2$," J. Appl. Phys. **37**(12), 4578–4580.

Pani, M., Merlo, F., and Fornasini, M. L. Z. (**2002**). "Structure and transport properties of the R_2Co_2Al compounds (R=Pr, Nd, Sm, Gd, Tb, Dy, Ho, Er, Tm, Y)," Z. Kristallogr. **217**, 415–419.

Riani, P., Freccero, R., Sufryd, K., Arrighi, L., and Cacciamani, G. (**2020**). "The 500 C isothermal section of the Al–Co–Nd ternary system," Phase Equilib. Diffus. **41**, 347–364.

Snyder, R. L. (**1992**). "The use of reference intensity ratios in X-ray quantitative analysis," Powder Diffr. **7**, 186–193.

Stegemann, F. and Janka, O. (**2018**). "Two series of rare earth metal-rich ternary aluminium transition metallides: rE_6Co_2Al (RE=Sc, Y, Nd, Sm, Gd–Tm, Lu) and $RE_6Ni_{2.25}Al_{0.75}$ (RE=Y, Gd–Tm, Lu)," Z. Naturforsch. **73**, 819–830.

Strnat, K. J. and Strnat, R. M. W. (**1991**). "Rare earth-cobalt permanent magnets," J. Magn. Magn. Mater. **100**, 38–56.

Szytula, A. and Leciejewicz, J. (**1994**). *Handbook of Crystal Structures and Magnetic Properties of Rare Earth Intermetallics* (CRC Press, London).

Tao, X., Ouyang, Y., Liu, H., Zeng, F., Feng, Y., Du, Y., and Jin, Z. (**2008**). "Ab initio calculation of the total energy and elastic properties of laves phase C15 Al_2RE (RE = Sc, Y, La, Ce–Lu)," Comput. Mater. Sci. **44**, 392–399.

Taylor, K. N. R. and Darby, M. I. (**1972**). *Physics of Rare Earth Solids* (Chapman & Hall, London).

Tougait, O. and Noël, H. (**2006**). "Crystal structures and magnetic properties of $NdCoAl_4$, $Nd_2Co_3Al_9$ and $Sm_2Co_3Al_9$," J. Alloys Compd. **417**, 1–6.

Walter, N. and Schreiner, A. (**1995**). "A standard test method for the determination of RIR values by X-ray diffraction," Powder Diffr. **10**, 25–33.

Weitzer, F., Hiebl, K., and Rogl, P. (**1989**). "Al, Ga substitution in RE_2Fe_{17} (RE=Ce, Pr, Nd): magnetic behavior of $RE_2Fe_{15}(Al,Ga)_2$ alloys," J. Appl. Phys. **65**, 4963–4967.

Xiao, Y. G., Huang, Q., Ouyang, Z. W., Lynn, J. W., Liang, J. K., and Rao, G. H. (**2006**). "Crystal and magnetic structures of laves phase compound $NdCo_2$ in the temperature range between 9 and 300 K," J. Alloys Compd. **420**, 29–33.

Yarmolyuk, P., Zarechnyuk, O. S., Aksel'Rud, L. G., Rykhal, R. M., and Rozhdestvenskaya, I. V. (**1986**). "Crystal structure of $Pr_7Co_6Al_7$ — a representative of the family $R_7Co_6Al_7$ (R=Pr, Nd, Sm)," Sov. Phys. Crystallogr. **31**(2), 230.

Young, R. A., Larson, A. C., and Paiva-Santos, C. O. (**2000**). *User's Guide to Program DBWS-9807a for Rietveld Analysis of X-Ray and Neutron Powder Diffraction Patterns with A PC and Various Other Computers* (School of Physics, Georgia Institute of Technology, Atlanta, Georgia).

Zeng, L., Qin, P., Qin, H., and Zhang, J. (**2007**). "Crystal structure and magnetic properties of the compound $FeDy_6Sb_2$," Mater. Lett. **61**, 300–303.